Advanced Composite Materials
Publication details, including instructions for authors and subscription information:
http://www.tandfonline.com/loi/tacm20

Comparative investigations on three-body abrasive wear behavior of long and short glass fiber-reinforced epoxy composites

Gaurav Agarwal[a], Amar Patnaik[a] & Rajesh Kumar Sharma[a]
[a] Mechanical Engineering, NIT Hamirpur, Hamirpur, India
Published online: 07 Jan 2014.

To cite this article: Gaurav Agarwal, Amar Patnaik & Rajesh Kumar Sharma (2014) Comparative investigations on three-body abrasive wear behavior of long and short glass fiber-reinforced epoxy composites, Advanced Composite Materials, 23:4, 293-317, DOI: 10.1080/09243046.2013.868661

To link to this article: http://dx.doi.org/10.1080/09243046.2013.868661

Advanced Composite Materials, 2014
Vol. 23, No. 4, 293–317, http://dx.doi.org/10.1080/09243046.2013.868661

Comparative investigations on three-body abrasive wear behavior of long and short glass fiber-reinforced epoxy composites

Gaurav Agarwal, Amar Patnaik* and Rajesh Kumar Sharma

Mechanical Engineering, NIT Hamirpur, Hamirpur, India

(*Received 22 July 2012; accepted 9 September 2013*)

The purpose of this investigation is to determine the three-body abrasive wear behavior of long and short E-glass fiber-reinforced epoxy composites in abrasive environment, subjected to designed experimental setup. A mathematical model for damage assessment in three-body abrasion is developed and validated by a well-designed set of experiments. The design of experiment using Taguchi's orthogonal array is applied to find out minimum specific wear rate. Steady state condition is also applied to find minimum specific wear rate for particular weight fraction keeping other parameters as constant. The experimental results show that the abrasive wear of the composites shows dependence on parameters like applied load, sliding speed, and abrasive particle size. Wear rate of long as well as short glass fiber-reinforced epoxy composites increases with increase in normal load and abrasive particle size, whereas the wear rate decreases up to 40 wt.% of fiber loading and then further increases with increase in sliding speed. The SEM micrograph studies reveal the dynamics of three-body abrasive wear and underlying micro-mechanisms that serve as determinant for wear performance of such composites. The three-body abrasive wear rate in given formulation increases with normal load and abrasive particle size. The mechanical characteristics observed a positive trend with the increase in fiber composition and also help in analyzing the specific wear rate of composites.

Keywords: composites; glass fiber; wear; mathematical model; Taguchi design

1. Introduction

The quest for the development of new and innovative material creates huge opportunity in the area of composite materials. Polymer matrix-reinforced composites containing different fibers and fillers are frequently used in applications like aerospace engineering, automotive part assembly, piping system for sanitation, ship hulls, and gear assembly used in every day applications. The high specific strength, stiffness, and light weight of polymers are primarily responsible for their popularity.[1–3] Abrasive wear of polymer matrix composite is a serious issue because repeated abrasion between two layers of polymer composites (two-body abrasion) or when loose particles are embedded in between two layers (three-body abrasion) causes loss of material. For effective working of fiber-reinforced polymer composites (FRPC's), abrasion wear is to be minimized. Three-body abrasions are in fact the most crucial and prominent in many applications. In order to reduce the amount of wear in a particular application, it is significant to correlate the wear performance behavior in relation to those operating parameters with

*Corresponding author. Email: amar_mech@sify.com

particular application demands. Glass fabric is produced by twisting and plying several strands of fibers. Long glass fiber (bidirectional) composites have two orientations (owing to two perpendicular directions of glass fiber) and hence can be oriented to support loads in two directions. Another significant advantage of using artificial fibers like glass fibers is that their dimensions might be precisely measured and monitored to obtain desired results throughout the length of the specimen.[4,5] The most commonly used matrix materials are epoxy or vinyl ester, and these are found to reinforce commonly with glass fiber, carbon fiber, and Kevlar fiber.[6] In case of three-body abrasive wear of short glass fiber polyester composites,[7,8] the size of abrasive particle, applied load, and sliding velocity observed to accelerate the wear loss. This is also observed to depend upon the type of fabric reinforcement and interphase temperature.[9] In case of two-body abrasive wear behavior of composite of glass/carbon fabric and vinyl ester, the wear loss is observed to accelerate with increase in the abrading distance/abrasive particle size. The composite having fibers at 0° (parallel to loading direction) proves best almost in all properties.[10–14]

The literature mentioned above reveals almost fewer attempt to investigate the three-body abrasion wear behavior of either of long and short glass fiber with epoxy resin. Therefore, the main aim of the presented research work lies in formulating long (bidirectional) and short (chopped) glass fiber-reinforced epoxy matrix-based polymer composite with different fiber loading and determining their wear behavior under a three-body abrasive environment. Finally, the experimental results are compared with the proposed mathematical model for validation purposes.

2. Mathematical model

In three-body abrasion, material is removed by the rubbing action of the two surfaces i.e. the rotating wheel (first body), the fixed specimen (second body), and the presence of loose abrasive particles (third body) in between these two surfaces. The amount of material removed and the specific wear rate in case of two-body and three-body abrasion methods are predicted by various scholars. The material loss is aided by processes such as micro-cutting, micro-ploughing, micro-cracking, and micro-fatigue resulting from abrasive wear. The models given by Rabinowicz [15] and Ratner et al. [16] relate the wear volume with sliding distance, normal load, hardness of the surface, coefficient of friction, and elongation to break. The Rabinowicz model [15] makes use of conical abrasive particles and correlate wear volume loss with the sliding distance and attack angle of the abrasive particle, this is given by

$$\frac{W_v}{s} = \frac{(2 \cdot tan\,\alpha) \cdot P}{H \cdot \pi} \tag{1}$$

where w_v = volume loss due to wear, S = sliding distance, P = normal load, H = hardness of the material, and α = attack angle.

According to Ratner et al. [16], the wear volume loss (V) in case of three-body abrasion for polymer-based composites is related to breaking stress (s), elongation to break (ε), coefficient of friction (μ), normal load (P), and hardness of the composite material (H); the relation is given as:

$$V = \frac{\mu \cdot C \cdot P}{H \cdot s \cdot \varepsilon} \tag{2}$$

where C is abrasive particles constant.

In the present work, we have introduced a predictive mathematical model for three-body abrasive wear akin to that proposed above by Rabinowicz and Ratner, respectively. In light of the studied literatures on mathematical modeling in context to three-body abrasive wear, the authors have proposed a new mathematical model for the computation of wear loss in three-body abrasion environment; the relations is:

$$\Delta W = \frac{\rho \cdot \mu \cdot P \cdot F \cdot L \cdot S}{H \cdot \varepsilon} \tag{3}$$

where F = percentage of fiber or fabric reinforcement, ρ = density of the material, L = length of fiber used, S = breaking strength, ε = elongation to break, H = hardness of the material, P = normal load, and μ = coefficient of friction. Henceforth, the modified form of specific wear rate relation appears as:

$$Ws_{th} = \frac{\mu \times F \times L}{H \times \varepsilon} \tag{4}$$

3. Experimental details

3.1. Specimen preparation

The polymer composite samples comprising of epoxy resin matrix reinforced with long (bidirectional) E-glass fabric (600 GSM) and short E-glass fiber (600 GSM, 5–8 mm length) are prepared with different weight percentages (10–50 wt.% in steps of 10%). The fabric/fibers (72.5 GPa, 2590 kg/m^3) are supplied by Saint Gobian and Hexcel Corporation, India, whereas epoxy resin (3.42 GPa, 1100 kg/m^3) and hardener are supplied by Ciba Geigy India Ltd. The epoxy (LY-556) and hardener (HY-951) are mixed in the ratio of 10:1 by weight as recommended by supplier, thereafter fabric/fibers are mixed properly by hand lay-up technique in moulds of appropriate size. The duration of approximately 48 h is provided for proper curing at room temperature. Thereafter, samples of appropriate dimensions were cut appropriate to physical, mechanical, and tribological studies.

3.2. Dry abrasion test rig

The experimental study of three-body abrasive wear behavior of the prepared composite samples was performed on DUCOM TR-50 dry abrasion test rig (Figure 1) following ASTM G65 standards. The abrasive particles are directed to flow from a hopper in between the specimen and the chlorobutyl rubber wheel (diameter: 228 mm) via a nozzle at the feeding rate of 255 ± 5 g/min^2. The experiments are carried out as per designed parameter mentioned in Table 1. The weights of the sample before and after the test are measured using high precision digital balance (Denver Instruments Germany, TB-2150) with an accuracy of ±0.1 mg. Each experiment run was repeated twice and the average value is reported. The specific wear rate (defined as the volume loss of the specimen per unit sliding distance per unit applied normal load) is expressed on 'volume loss' basis as,

$$W_s = \frac{\Delta m}{\rho.t.V_s.F_n} \tag{5}$$

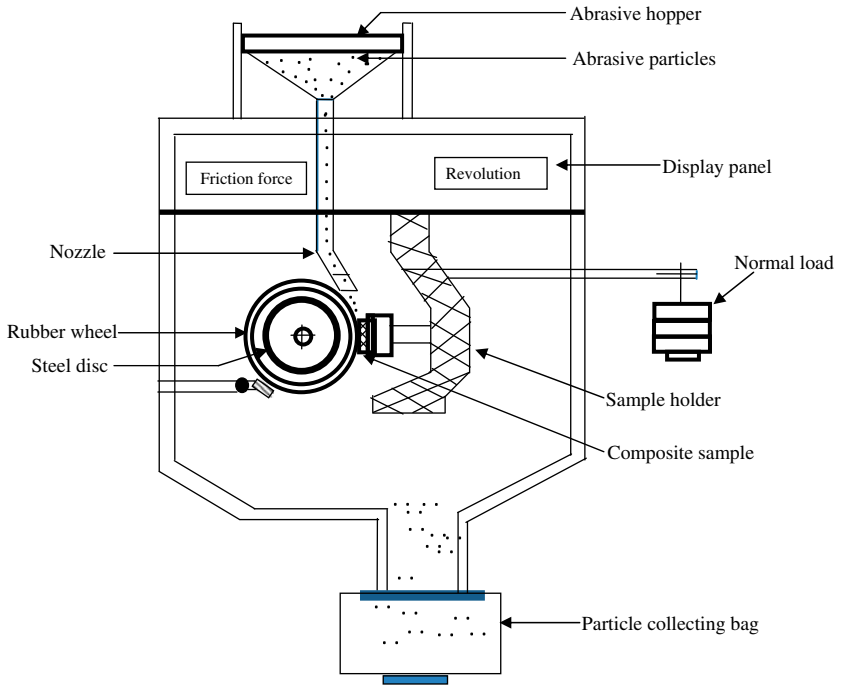

Figure 1. Experimental setup for abrasive wear test rig.

Table 1. Levels of the variables used in the experiment.

	Levels					
Control factors	I	II	III	IV	V	Units
Sliding velocity	48	72	96	120	144	cm/s
Fiber loading	10	20	30	40	50	wt.%
Normal load	20	40	60	80	100	N
Sliding distance	50	60	70	80	90	m
Abrasive size	125	250	375	500	625	μm

where W_S is the specific wear rate (mm^3/Nm), Δm is the mass loss under specified test duration (g), ρ is the density of the composites (g/mm^3), t is the test duration (s), V_s is the sliding velocity (m/s), and F_n is the average normal load (N).

3.3. *Physical and mechanical characterization*

The fabricated composites are characterized for their physical as well as mechanical properties. The theoretical density of the samples is computed using a relation proposed by Agarwal and Broutman [17] i.e.

$$\rho_{ct} = \frac{1}{\frac{W_f}{\rho_f} + \frac{W_m}{\rho_m}} \tag{6}$$

where W_f and W_m are the weight fraction of fibers and matrix, respectively; ρ_{ct}, ρ_f, and ρ_m are the density of the composite material, fiber, and matrix resin, respectively. The experimental density (ρ_{ex}) is measured by simple water immersion technique. Thereafter, void fraction (Δv) is computed by normalizing the differences in both densities against the theoretical density i.e.

$$\Delta v = \left[\frac{\rho_{ct} - \rho_{ex}}{\rho_{ct}}\right] \tag{7}$$

The tensile strength, flexural strength, and interlaminar shear strength (ILSS) are evaluated on universal testing machine Instron 1195. Specimen dimensions for the tensile test are 150 mm × 15 mm × 15 mm in accordance with ASTM D 3039-79,[18] similarly for flexural test specimen dimensions are 150 mm × 15 mm × 15 mm, span length of 50 mm at cross head speed of 2.54 mm/min in accordance with ASTM D 2344-84 (ASTM D 256-97, 1984), while for ILSS [19] the specimen dimensions are 75 mm × 15 mm × 15 mm, span length of 30 mm at cross head speed of 2.54 mm/min is taken. For impact testing, a plastic impact tester following ASTM D256 (ASTM D 256-97, 1999) of dimensions 64 mm × 12.7 mm × 3.2 mm with 45° V-shaped groove at 2 mm depth is used.[20]

Micro-hardness measurement is done using a Leitz micro-hardness tester, equipped with a square-based pyramidal (angle 136° between opposite faces) diamond indenter by applying a load of 24 N. Vickers hardness number is calculated using the following equation:

$$H_v = 0.1889 \cdot \frac{F}{L^2} \text{ and } L = \frac{X + Y}{2} \tag{8}$$

where H_v is the hardness, F is the applied load, L is the diagonal of the square impression, and X and Y are the two diagonals of the diamond indenter. The surface morphology studies are performed on SEM CARL ZEISS NTS GMBH, SUPRA 40VP. The specimens were gold coated in order to enhance the conductivity of the samples, thereafter micrographs are taken for detail study of dynamics of wear mechanism.

3.4. *Experimental design*

Experimental design using Taguchi method is a technique to reduce the number of iterations and to effectively obtain the optimal result. This technique has been utilized widely in engineering analysis to optimize the performance characteristics with the combination of design parameters. The Taguchi method obtains the optimal condition by reducing the number of trials (iterations) for the particular combination. Here, Taguchi experimental method is planned for five factors and five levels. Table 1 indicates the factors selected for experimental analysis using Taguchi method. The array chosen was the L_{25} which has 25 rows corresponding to the number of variables selected. In Table 1 each column denotes a test parameter, whereas row denotes the combination of parameter selection by Taguchi technique. The experimental outputs are further converted into signal to noise (S/N) ratio. In S/N analysis, the lesser the S/N ratio, the better are the experimental results to reduce the wear rate of the composites. However, there are three categories of quality check up i.e. lower-the-better, higher-the-better, and nominal-the-better; therefore, to obtain optimal characteristics for wear rate lower-the-better must be taken.

$$\text{Smaller-the-better characteristic:}\frac{S}{N} = -10\log\frac{1}{n}\left(\sum_{i=2}^{n} y^2\right) \tag{9}$$

After studying the experiment, a statistical analysis of variance (ANOVA) tool was used to identify the process parameters that are statistically useful with S/N and ANOVA analysis and the optimal combination of the process parameters can be predicted to the desired level.

4. Results and discussion

The first section discussed the physical and mechanical properties of glass fiber (bidirection/chopped short glass fiber)-reinforced epoxy composites and its overview. The second section mainly discussed the interpretation of experimental results for both the fiber loading and comparison with the proposed mathematical model. Finally, we have discussed the significance of factor settings and their effect on specific wear rate of the composites.

4.1. Physical and mechanical properties

4.1.1. Effect of void content on bidirection/chopped short glass-epoxy composites

The comparison between theoretical and experimental density of composites is shown in Table 2. As the density of fiber reinforcement increases, the volume fraction of void also tends to increase. The presence of void directly or indirectly affects the mechanical properties of composites.

4.1.2. Effect of hardness on bidirection/chopped short glass-epoxy composites

It is seen that hardness first decreases from 10 to 30 wt.% fiber reinforcement and then increases for 40 and 50 wt.% fiber content (Figure 2). The decrease in hardness is due to the presence of pores and voids. However, the expected hardness values of (bidirectional and chopped) fiber composites increase with the increase in the percentage of reinforcement.

Table 2. Comparison between experimental density and theoretical density.

S. no.	Composite composition	Experimental density (ρ_{ex}) g/cm^3	Theoretical density (ρ_{ct}) g/cm^3	Void fraction $\Delta v = \left[\frac{\rho_{ct}-\rho_{ex}}{\rho_{ct}}\right]$
1	Epoxy + 10% Glass Fabric (L)	1.254	1.26	0.48
2	Epoxy + 20% Glass Fabric (L)	1.384	1.392	0.58
3	Epoxy + 30% Glass Fabric (L)	1.422	1.431	0.63
4	Epoxy + 40% Glass Fabric (L)	1.508	1.529	1.39
5	Epoxy + 50% Glass Fabric (L)	1.597	1.642	2.82
6	Epoxy + 10% Glass fiber (S)	1.258	1.265	0.56
7	Epoxy + 20% Glass fiber (S)	1.331	1.339	0.60
8	Epoxy + 30% Glass fiber (S)	1.413	1.422	0.64
9	Epoxy + 40% Glass fiber (S)	1.491	1.515	1.61
10	Epoxy + 50% Glass fiber (S)	1.58	1.622	2.66

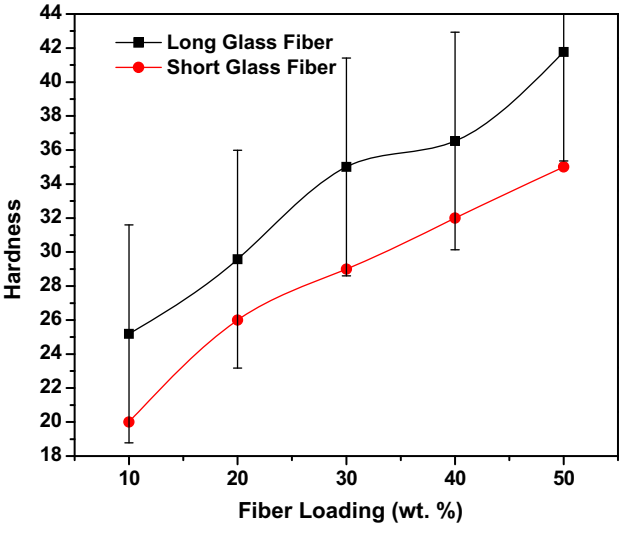

Figure 2. Effect of fiber loading on hardness of the composites.

4.1.3. *Effect of tensile strength on bidirection/chopped short glass-epoxy composites*

Figure 3 shows that tensile strength of Bidirectional E-glass fabric-reinforced epoxy composites increases with the increase in the percentage of fabric content, except that for 30 wt.% fabric content. This increase may be due to the fact that as the layers of bidirectional fabric increases with the increase in fabric wt.%, more strength is obtained and better bonding is achieved between the surface of fabric and epoxy resin. Also long fibers weaved in the form of fabric help in transferring loads effectively to enhance tensile strength. For chopped E-glass fiber-reinforced epoxy composites, tensile strength shows a linear behavior. The possibility is that the fibers are short (5–8 mm) in length and may not transfer tensile stress effectively. Similarly, observations were proposed by Stokes [21] and Thomason and co-workers [22] for random glass FRPCs tensile strength results. The decrease in tensile strength with the increase in fiber loading may be due to inhomogeneity of fibers arranged in the matrix material and also the influence of fiber length and concentration on the properties of glass fiber reinforcement.

4.1.4. *Effect of flexural strength on bidirection/chopped short glass-epoxy composites*

Test results of Flexural strength are shown in Figure 4. The flexural strength of the bidirectional glass fiber-reinforced epoxy composites increased with the increase in fiber loading up to 30 wt.% (>150 MPa). However, on further increase in fiber loading i.e. up to 50 wt.%, the bending strength of the composites starts decreasing in case of bidirectional glass fiber composites (>120 MPa). The decrease in flexural strength may be due to higher void fraction (as reported in Table 2) in higher fiber loading or it may be caused by weak fiber-to-fiber interaction and dispersion. Similarly, observations were reported by Asri and Khalil [23] that the lower flexural strength of the thermoplastic composites might be attributed to the low interaction and poor dispersion of the fiber in the matrix. However, in case of chopped short glass fiber-reinforced epoxy composites,

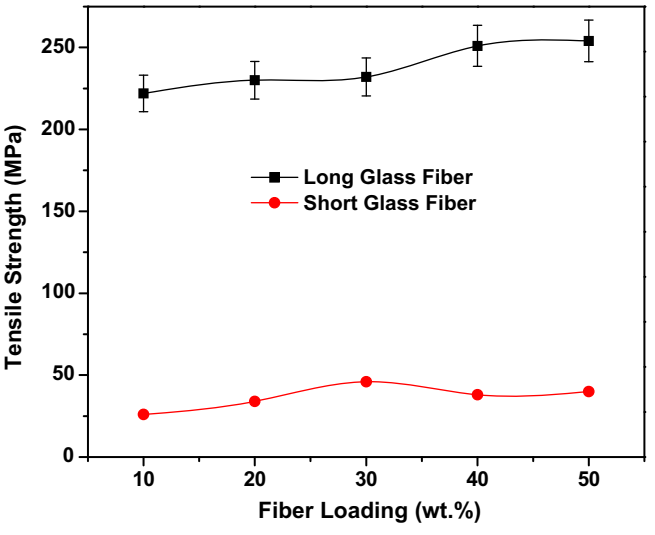

Figure 3. Effect of fiber loading on tensile strength of the composites.

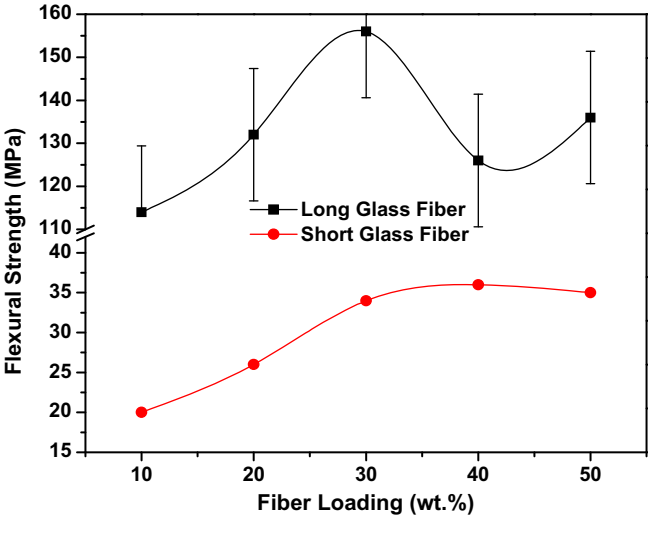

Figure 4. Effect of fiber loading on flexural strength of the composites.

the flexural strength of the composites showed similar trends similar to bidirectional glass fiber-reinforced epoxy composites but with lower flexural strength (Figure 4). In chopped short fiber composites the flexural strength is increased up to 40 wt.% fiber loading (Figure 4). But on further increase in fiber loading, the flexural strength starts decreasing in trend. Therefore, from this observation it is clear that for structural application the fabrication of bidirectional glass fiber an increase up to 30 wt.% fiber loading for high strength applications is proposed and for low strength applications an increase

up to 40 wt.% loading for chopped short fiber-reinforced epoxy composites is advisable.

4.1.5. Effect of ILSS and impact strength of bidirection/chopped glass-epoxy composites

ILSS is a useful test for composites where the chances for failure of lamina initiate when subjected to shearing stresses. ILSS for bidirectional fabric as well as chopped fiber shows a similar increase in strength with the increase in the percentage of fiber content (Figure 5). The values of chopped fiber are slightly less than that of bidirectional fabric. The increase in ILSS may be an effective use of fiber strength being dependent on both the interfacial adhesion properties and the critical fiber length. Nigel and Brown [24] reported similar results for glass fiber-reinforced phenolic resin composites with ILSS. As ILSS of composites mainly depends on two major factors i.e. base material strength and composite void content. In this study, both the bidirectional and chopped glass fiber-reinforced epoxy composites show linear increase in ILSS (Figure 5). However, for similar composites as far as void fraction is concerned (as observed from Table 2), it increases with the increase in fiber loading. Therefore, it is an obvious phenomenon that with the increase in void fraction the mechanical strength may decrease. But from this analysis it shows a reverse trend. However, Nigel and Brown [24] also reported that the effects of voids depend on their size present in the composites. The larger voids generally acted as crack initiation direction under a shear stress, whereas the increase in stress due to the reduction in net cross-sectional area was the main factor in shear failure of composites with smaller distributed voids in the composites. Similar observation is also observed in case of impact strength of the bidirectional and chopped short glass fiber-reinforced epoxy composites as shown in Figure 6. Readings show that the resistance to impact loading of bidirectional and chopped fiber composites improves by increasing fiber percentage. However, this

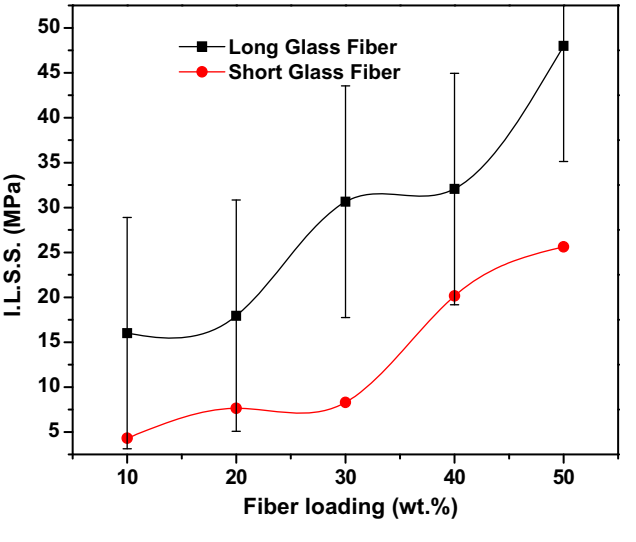

Figure 5. Effect of fiber loading on ILSS of the composites.

improvement is not very significant because higher impact loads may be required in modern engineering applications. Therefore, from this analysis it was concluded that the results on mechanical properties of bidirectional glass fiber-reinforced epoxy composites denote a significant effect in mechanical properties with the increase in the percentage of reinforcement, whereas chopped glass fiber epoxy composites do not show significant improvement in mechanical properties with that of percentage of reinforcement material.

4.2. *Steady state specific wear*

4.2.1. *Effect of sliding velocity on wear rate of bidirectional glass fiber composites*

Abrasive wear tests were conducted to find the effect of change in wear rate with the change in rotation speed of a rubber wheel. Rotation speed vary in steps of 20 rpm from a minimum value of 40 rpm to a maximum value of 120 rpm keeping other parameters i.e. normal load as 40 N, sliding distance 60 m, and abrasive particle size 375 μm as constant. Figure 7(a) represents the effect on wear rate with the change in sliding velocity. Wear rate decreases with the increase in sliding velocity; wear rate is maximum at 10 wt.% glass fiber composition then linearly decreases till 30 wt.%, Then remain constant between 30 and 50 wt.% fiber composition of glass fiber composites. This is due to the fact that at 10 wt.% glass fiber the composition of resin is 90 wt.% i.e. due to higher percentage of matrix material the wear rate is more. We know from the discussion of mechanical properties that increase in fiber loading improves the mechanical properties and hence reduces wear. Similarly, as the percentage of glass fiber increases, matrix material (epoxy) reduces and hence there is an increase in mechanical properties and therefore less amount of wear occurs. From 30 wt.% till 50 wt.% the wear rate is constant because further increment in sliding speed may not affect the wear rate further (Figure 7(a)).

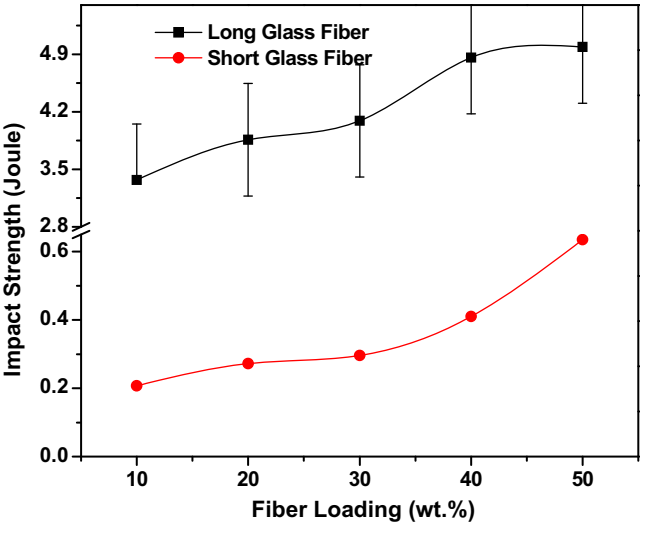

Figure 6. Effect of fiber loading on impact strength of the composites.

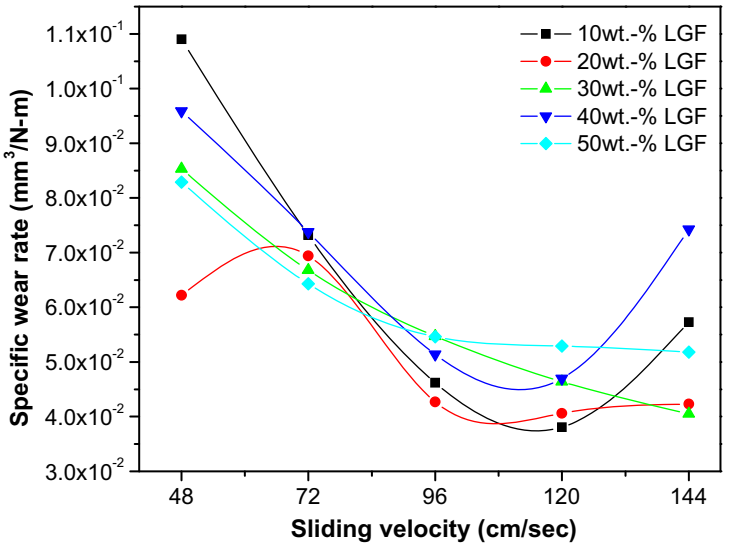

Figure 7a. Effect of sliding velocity on specific wear rate of the long glass fiber-reinforced epoxy composites (At constant normal load: 40 N, sliding distance: 60 m, and abrasive size: 375 μm).

4.2.2. Effect of normal loading on wear rate of bidirectional glass fiber composites

Steady state abrasive wear tests were conducted to study the effect of change in wear rate with the change in normal load. Normal load varies in a step of 20 N from minimum value of 20 N to maximum value of 100 N and keeping other parameters such as sliding speed: 72 m/s, sliding distance: 60 m, and abrasive size: 375 μm constant. Figure 7(b) shows the effect of change in normal load with the change in

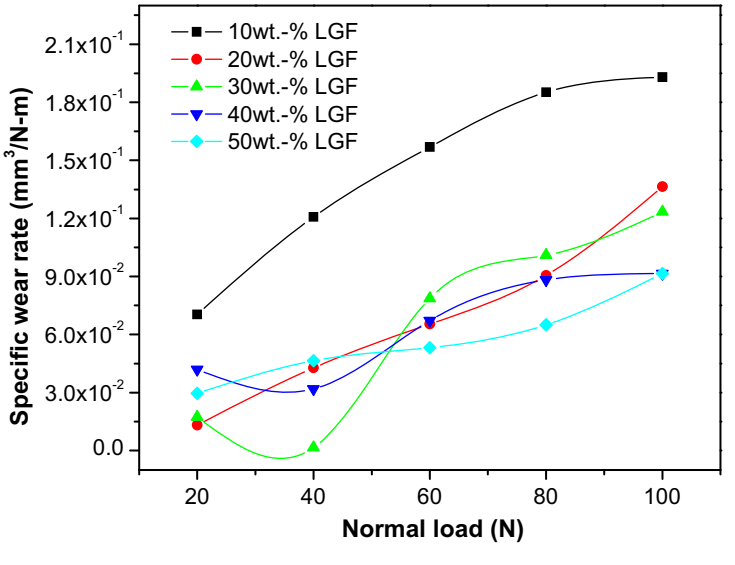

Figure 7b. Effect of normal load on specific wear rate of the short glass fiber-reinforced epoxy composites (At constant sliding velocity: 72 cm/s, sliding distance: 60 m, and abrasive size: 375 μm).

wear rate of bidirectional glass fiber-reinforced epoxy composites. Wear rate increases with the increase in normal load for all the fiber loading ratio because as the normal load increases for a specimen, more surface of specimen is in contact with free flowing abrasive particles and rotating wheel and in turn removes more amount of material and thereby increases wear rate of the composites.

4.2.3. *Effect of sliding velocity on wear rate of chopped fiber composites*

Variation in wear rate with sliding speed is shown in Figure 8(a). As the sliding speed increases, wear rate for the chopped glass fiber-reinforced epoxy composites decreases because at higher rotation speed surface contact between the rubber wheel and the specimen reduces and therefore less number of abrasive particles embedded inside the surface of the rubber wheel which in turn removes less amount of material. As shown in Figure 8(a), at 20 wt.% fiber loading wear rate reduces exceptionally when compared with other composites. The reduction in wear rate is probably due to poor fiber-matrix combination and there may be chances of weak interfacial bonding.

4.2.4. *Effect of normal loading on wear rate of chopped fiber composites*

Figure 8(b) shows that wear rate increases with the increase in normal load (N) of the composites. As the normal load increases more amount of pressure is induced on the surface of the specimen and hence particles present in between get embedded inside the surface which removes huge amount of material because the rotation speed of the rubber is lower. Wear rate at 100 N is more in almost all the composites but among the fiber reinforcement 10 wt.% fiber loading shows maximum wear rate (Figure 8(b)). It is

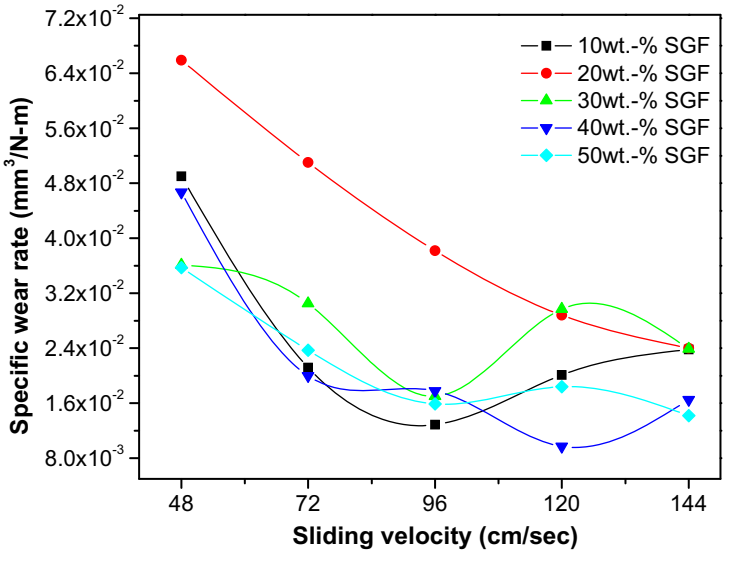

Figure 8a. Effect of sliding velocity on specific wear rate of the short glass fiber-reinforced epoxy composites (At constant normal load: 40 N, sliding distance: 60 m, and abrasive size: 375 μm).

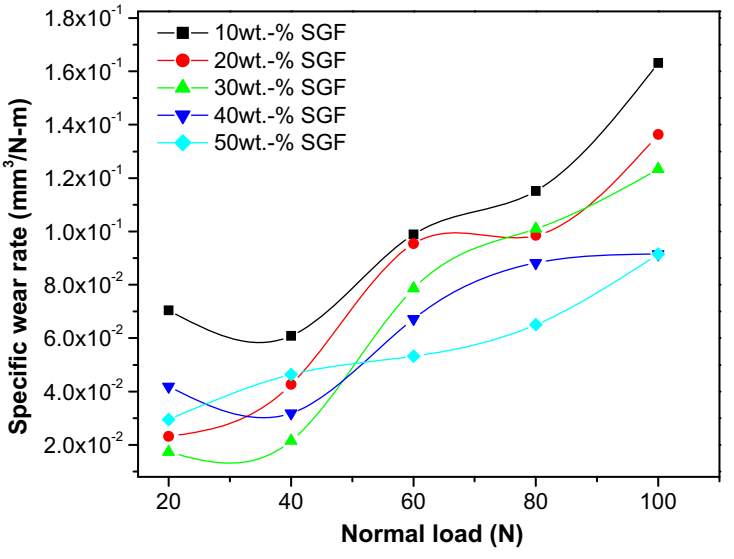

Figure 8b. Effect of normal load on specific wear rate of the short glass fiber-reinforced epoxy composites (At constant sliding velocity: 72 cm/s, sliding distance: 60 m, and abrasive size: 375 μm).

also observed in this study that with the increase in fiber loading the wear resistance increases gradually with increase in normal load.

4.3. Thermo-mechanical properties of composite (dynamic mechanical analysis)

The viscoelastic responses of the composites were measured using dynamic mechanical analysis (DMA), conducted in a nitrogen atmosphere at a fixed frequency of 1 Hz, heating rate of 2 °C/min, temperature range 29–250 °C, and at a strain of 1% on rectangular samples with approximate sample dimensions of 40.000 × 12.000 × 4.0 mm using NETZSCH DMA 242 instrument in bending mode.[25,26]

Analysis is performed to calculate damping capacity of the material during mechanical vibrations under cyclic loading. Thus, high damping capacity of the material absorb vibrations, which in turn is used to reduce noise and for the stabilization of the structure. Studies have been carried out on to notice the effect of thermo-mechanical properties using DMA instrument on long and short glass fiber-reinforced epoxy composites. DMA studies have been carried out for each weight percent of long and short glass fiber-reinforced epoxy composite to notice the variation of loss modulus (E''), storage modulus (E'), and damping parameter ($\tan\delta$) as a function of temperature as shown in Figures 9(a–c). Damping factor ($\tan\delta$) is then a ratio of storage modulus to loss modulus for each composition i.e.

$$\tan\delta = \frac{E'}{E''}$$

In Figure 9(a), the loss modulus verses temperature graph shows the no recoverable vibrational energy. With the increase in the value of temperature from 0 to 60 °C, value

of loss modulus slightly increases, whereas from 60 to 100 °C the value of loss modulus attains a peak value which further decreases rapidly with the increase in temperature up to 100 °C, increasing the value of temperature beyond 100 °C. The value of loss modulus almost attains a straight line i.e. slight decrease in the value of loss modulus is noticed with the increase in the value of temperature. For bidirectional glass fiber-reinforced epoxy composites, values of loss modulus follow a trend i.e. $E'_{10} > E'_{50} > E'_{20} > E'_{40} > E'_{30}$, whereas values of loss modulus for short carbon fiber-reinforced epoxy composite follow a trend that $E'_{30} > E'_{40} > E'_{50} > E'_{10} > E'_{20}$. This may be due to the behavior of fiber content and resin bonding with that of temperature leading to increase or decrease in height and peak width. Further it has also been observed that for the composites with lower fiber content the shift in the loss peak is more towards higher temperature.[27] This can be clearly verified from Figure 9(a) i.e. for 10 wt.% bidirectional GFRE composites peak value of loss modulus is more than that for 30 wt.% GFRE composites; similar observations are obtained for short GFRE composites where the peak value at 30 wt.% fiber loading is higher than that at 50 wt.% fiber loading. While comparing the loss modulus characteristics for long and short GFRE composites, the values for long GFRE composites are exceptionally higher than that for short GFRE composites. This is because due to weave pattern bidirectional GFRE composites provide higher strength than that of short GFRE composites.

Figure 9(b) shows a graph of storage modulus vs. temperature for long and short GFRE composites. From room temperature to 65 °C storage modulus, values are nearly constant for bidirectional and short GFRE composites. Region 1 shows a glassy regime in the range of 0 to 65 °C in this region with no appreciable change in the properties of storage modulus being noticed corresponding to change in the value of temperature, whereas region 2 shows a sharp decline in the values of storage modulus between 65 and 100 °C i.e. the material changes from glassy to rubber transition regime with the increase in the values of temperature from 65 to 110 °C. Region 3 again is a straight line with a slight increase or decrease in the value of storage modulus noticed between 110 and 250 °C and the values nearly tend to zero, which shows a rubbery regime indicating degradation of the moduli above 110 °C. Values of storage modulus for

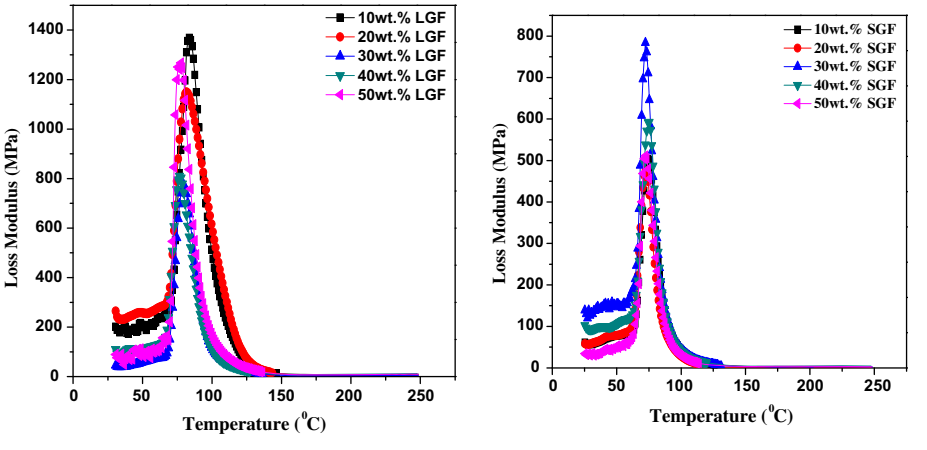

Figure 9a. Variation of loss modulus with temperature for long and short glass fiber-reinforced epoxy composites.

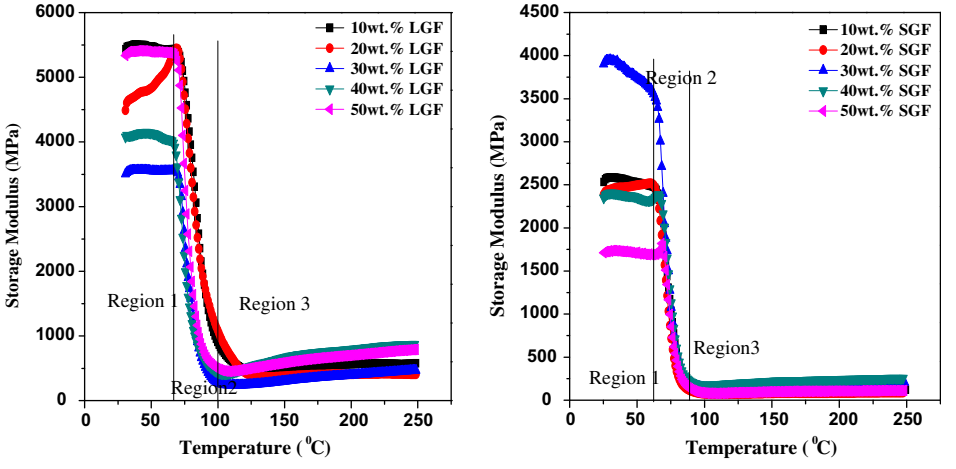

Figure 9b. Variation of storage modulus with temperature for long and short glass fiber-reinforced epoxy composites.

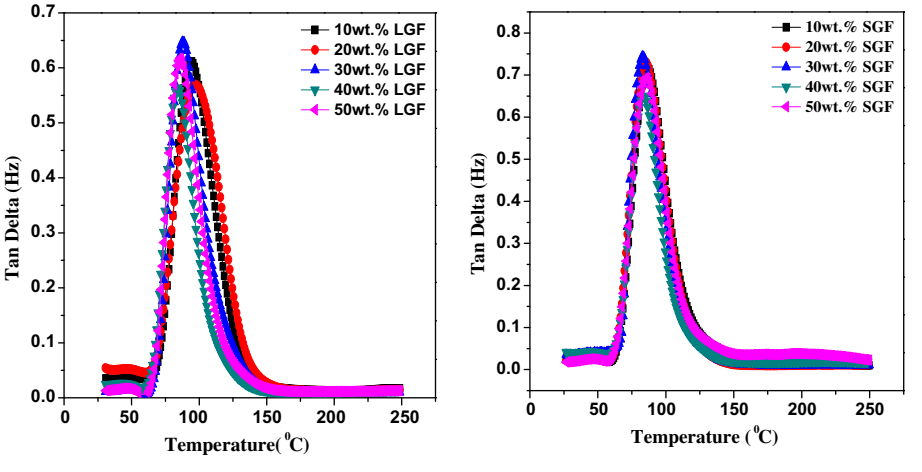

Figure 9c. Variation of tan δ with temperature for long and short glass fiber-reinforced epoxy composites.

bidirectional GFRE composites are exceptionally higher than that of short GFRE composites and the transition from glassy to rubbery regime is faster in short GFRE composites than that of bidirectional GFRE composites; this may be due to the certain weave pattern noticed in bidirectional GFRE composites and due to which the thermomechanical properties as well as transformation regime is longer for bidirectional composites than that for short GFRE composites. The higher values in region 1 and sharp decrease in the values in region 2 are due to the fact that in region 1 the material is in a glassy state in which the contribution of elastic modulus is more than the viscous modulus, whereas in region 2 the material is in glass transition stage in which a change from glass state into rubber-elastic state takes place. When the time scale of molecular

motion coincides with that of mechanical deformation, each oscillation is converted into the maximum possible internal friction and nonelastic deformation. In the glass transition region, the storage modulus falls during heating to a level of one-thousandth to ten-thousandth of its original value.[26] However, at elevated temperature region 3 (rubbery region), there is a slight improvement in the value of storage modulus.

Figure 9(c) shows the behavior of damping factor for bidirectional and short GFRE composites with the increase in the temperature of the composite. The peak value of $\tan\delta$ indicates that the material is nonelastic, whereas the lower value of $\tan\delta$ indicates that the material is elastic in nature. The highest peak value of $\tan\delta$ for 50 wt.% bidirectional composite shows that the material is nonelastic in nature, whereas the lowest peak value of $\tan\delta$ for 10 wt.% bidirectional composite shows that the material is elastic.

4.4. *Analysis of experimental results by Taguchi experimental design*

In Table 3, the eight and tenth columns represent *S/N* ratio of the specific wear rate of the composites which is in fact the average of two replications. The overall mean for the S/N ratio of the specific wear rate is found to be 24.96 db for bidirectional glass fiber-reinforced epoxy-based composites and 25.57 db for the chopped glass

Table 3. Experimental design using L_{25} orthogonal array.

Expt. no.	Sliding velocity (cm/s)	Fiber loading (wt.%)	Normal load (N)	Sliding distance (m)	Abrasive size (μm)	Ws (L) mm^2/ N cm	S/N Ratio (L) (db)	Ws (S) mm^2/ N cm	S/N ratio (S) (db)
1	48	10	20	50	125	0.03952	28.0637	0.03124	30.1058
2	48	20	40	60	250	0.06396	23.8818	0.04843	26.2977
3	48	30	60	70	375	0.07448	22.5592	0.07324	22.7050
4	48	40	80	80	500	0.10306	19.7382	0.05962	24.4922
5	48	50	100	90	625	0.09104	20.8154	0.08738	21.1718
6	72	10	40	70	500	0.06810	23.3371	0.01672	35.5353
7	72	20	60	80	625	0.06119	24.2664	0.03912	28.1520
8	72	30	80	90	125	0.12730	17.9034	0.14140	16.9910
9	72	40	100	50	250	0.09359	20.5754	0.05954	24.5038
10	72	50	20	60	375	0.03962	28.0417	0.04105	27.7337
11	95	10	60	90	250	0.02277	32.8527	0.02591	31.7307
12	95	20	80	50	375	0.05918	24.5565	0.03554	28.9857
13	95	30	100	60	500	0.03718	28.5938	0.04605	26.7354
14	95	40	20	70	625	0.03552	28.9905	0.04226	27.4814
15	95	50	40	80	125	0.16520	15.6398	0.14690	16.6596
16	119	10	80	60	625	0.01469	36.6596	0.01974	34.0931
17	119	20	100	70	125	0.06749	23.4152	0.05404	25.3457
18	119	30	20	80	250	0.04537	26.8646	0.05763	24.7870
19	119	40	40	90	375	0.06805	23.3434	0.11832	18.5388
20	119	50	60	50	500	0.08805	21.1054	0.07043	23.0448
21	143	10	100	80	375	0.01343	37.4385	0.02745	31.2292
22	143	20	20	90	500	0.02249	32.9602	0.02672	31.4633
23	143	30	40	50	625	0.08023	21.9133	0.09312	20.6191
24	143	40	60	60	125	0.13412	17.4501	0.11688	18.6452
25	143	50	80	70	250	0.06980	23.1229	0.07595	22.3894

Note: *Ws* (L): Specific wear rate for long glass fiber reinforced epoxy composites.
Ws (S): Specific wear rate for short glass fiber reinforced epoxy composites.

fiber-reinforced epoxy-based ones. The analysis was made using the popular software used for design of experiment applications known as MINITAB 15. From this analysis it is observed that the erosive result leads to the conclusion that factor combination of A_1, B_3, C_1, D_5, and E_1 gives minimum specific wear rate (Figure 10(a)) for bidirectional glass-epoxy composites, and for chopped glass-epoxy composites the factor combination of A_3, B_3, C_1, D_3, and E_1 gives minimum specific wear rate (Figure 10(b)). Table 3 presents the specific wear rate of bidirectional glass-epoxy composites and compares them with the results for chopped glass-epoxy composites. It is observed that for similar test conditions chopped glass-epoxy composites exhibit much lower wear rates than those for bidirectional glass-epoxy composites. This establishes chopped glass-epoxy as a better candidate for reinforcement as compared to bidirectional glass-epoxy from a wear response point of view.

4.5. Surface morphology

When a rubber wheel moves against the surface of the work piece, a loose abrasive particle (silica sand) abrades the surface, and after 'n' turns material is removed on the composite surfaces and wear occurs. Figure 11(a) shows a portion of bidirectional E-glass fabric after three-body abrasive wear, wear scars on the surface indicate that wear is in the direction of movement of the rubber wheel (longitudinal direction) (See Table 3, Expt. 1 and Column 8). From Figure 11(a) it is also observed that the amount of material removal is less as observed from Table 3 and Expt. 1. This may be due to that (i.e. 125 μm) abrasive particle unable to penetrate into the composite surface because of small size. Therefore, less penetration and less number of abrasive particles were in action with the rubbing surface resulting in low wear. However, with increase

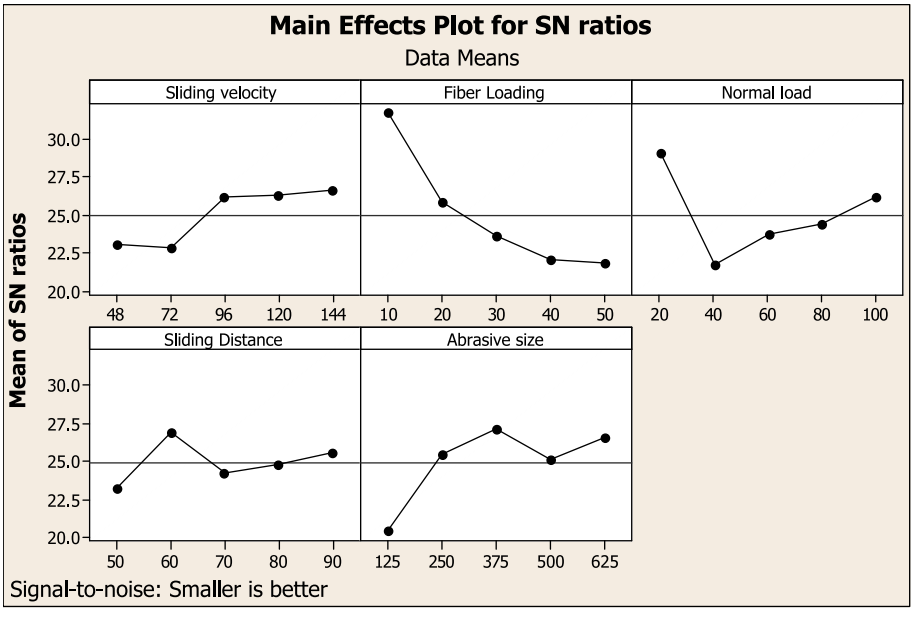

Figure 10a. Effect of control factors on signal-to-noise ratio of long glass fiber-reinforced epoxy composite.

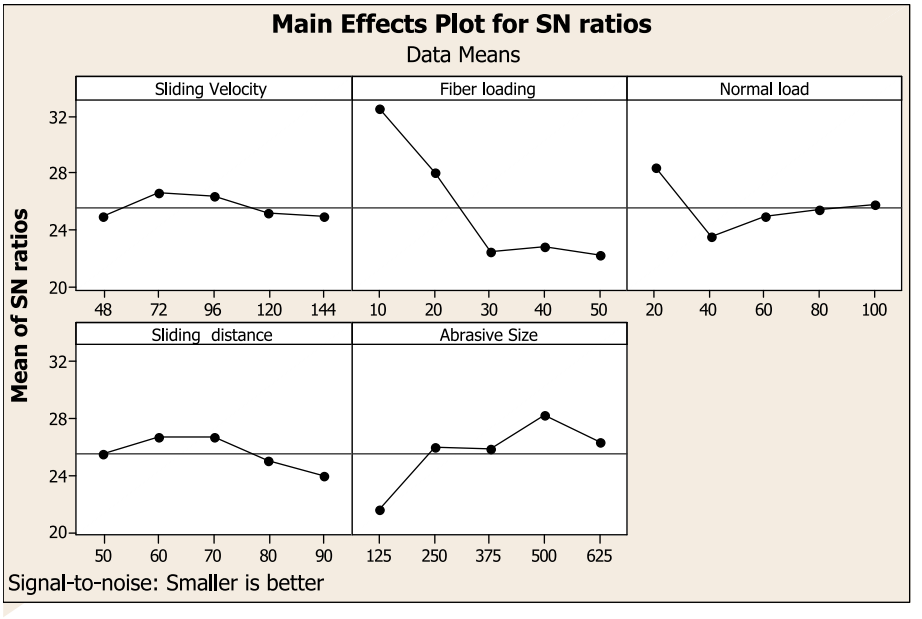

Figure 10b. Effect of control factors on signal-to-noise ratio of short glass fiber-reinforced epoxy composite.

in abrasive particle size the wear rate of the bidirectional glass fiber epoxy composite increases. Figure 11(b) denotes the abraded surface of bidirectional glass fiber composites with 20 wt.% fiber loading, due to three-body abrasive wear longitudinal fibers being removed and transverse fibers exposed on to the surface (Table 3, Expt. 1 and Column 8). The fibers are removed from the upper surface of the composites due to the presence of pores and voids. As the presence of pores and voids reduce the wear resistance of the composites and affect the proper leveling of the composite surface. Figure 11(c) shows the protrusion of loose fibers on upper surface of the chopped E-glass fiber-reinforced epoxy composite. Surface details show that short fibers are present randomly in all the directions inside the composite specimen (Table 3, Expt. 1 and Column 10) and wear loss is slightly lower then the bidirectional glass fiber-reinforced composites. This may be due to the fibers being randomly orientated inside the matrix material. For low sliding velocity (48 m/s), low fiber loading (10 wt.%), and low abrasive particle size (125 μm), the amount of matrix material loss from the composite is also less. However, with increase in sliding velocity and abrasive particle size, the material removal from the upper surface of the composite may increase automatically.

On the other hand, with the increase in sliding velocity (72 m/s) and erodent size (625 μm), the stress concentrated load on the composite also increases which in turn could fracture the chopped fiber-reinforced epoxy composites as shown in Figure 11(d) (Table 3, Expt. 7, and Column 10). However, with similar operating conditions, the bidirectional glass fiber-reinforced epoxy composites show more wear rate as compared with chopped glass-epoxy composites as seen in Figure 11(e) (Table 3, Expt. 7 and Column 8). This may be due to larger size sand particles (625 μm) exhibiting high stress concentration compared to the smaller sized abrasive sand particle. However, under similar sliding velocity (72 m/s) but lower abrasive particle size (125 μm), the

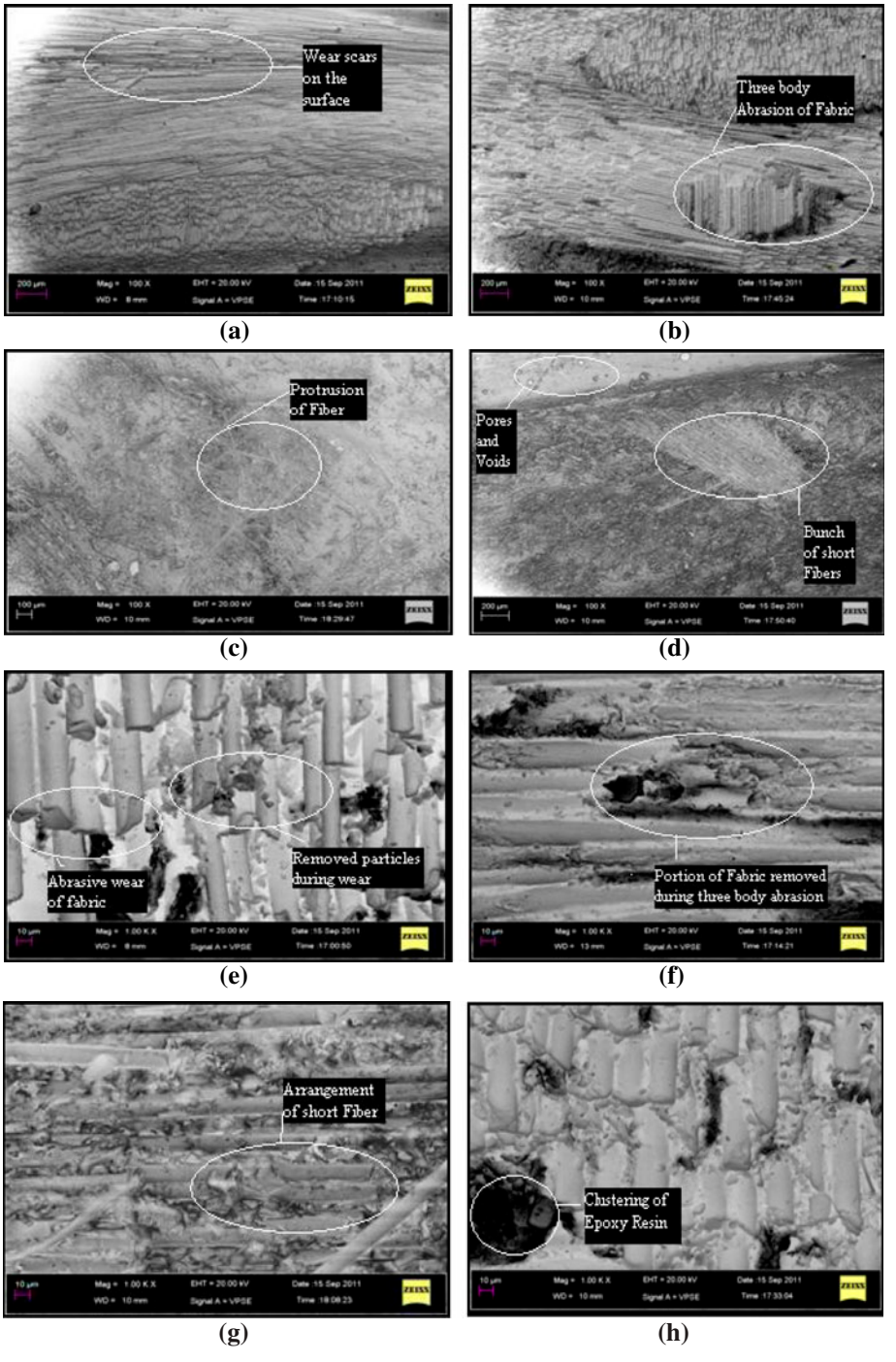

Figure 11. SEM micrograph of abraded surface of long/short glass fiber-reinforced epoxy composites.

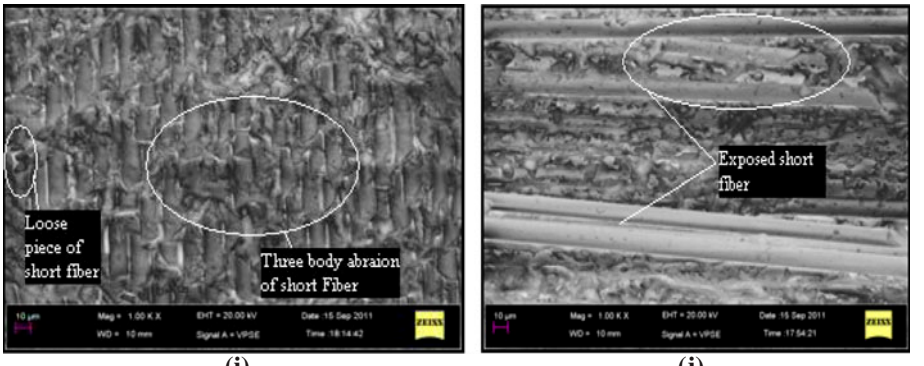

Figure 11. (*continued*)

abrasive wear behavior is automatically reduced to four to five times as shown in Figure 11(f) (See Table 3, Expt. 8 and Column 8) for bidirectional glass-epoxy composites. Similarly, for chopped fiber-reinforced epoxy composite under similar operating conditions (See Table 3, Expt. 8 and Column 10), the variation of matrix removal remains same (Figure 11(g)). However, on further increase in sliding velocity to 120 m/s, the clogging of wear debris generated during the sliding lead to higher matrix material removal on the bidirectional glass-epoxy composites where the predominant wear mechanisms are fiber detachment, pitting, macro-cracks etc. (Figure 11(h)). The degree of penetration is slightly higher compared to Figure 10f (See Table 3, Expt. 16 and Column 8), which eventually leads to fiber detachment from the composite surface and to large amount of matrix degradation taking place in the composites. This can be clearly evident from Figures 11(i and j) (See Table 3, Expt. 23 and Column 8 and 10) for higher sliding velocity (144 m/s) and higher abrasive size (625 μm). In the above operating conditions, both the bidirectional and chopped glass-epoxy composites exhibit similar specific wear rate as compared to other operating conditions (See Table 3, Expt. 23 and Column 8 and 10).

4.6. Calculations of theoretical results and comparison with experimental results

The developed theoretical predictive results of specific wear rate (*Ws*) of bidirectional/chopped glass fiber-reinforced epoxy composites are calculated using Eq. 4. From the equation it is evident that specific wear rate is directly proportional to coefficient of friction, percentage of fiber reinforcement, and length of fiber, whereas inversely proportional to hardness of the composite and percentage length for elongation to break of fiber. Here, length of fabric (L) for long E-glass fabric is 20 cm as the composites are prepared for 20 mm length × 20 mm width, whereas the elongation to the selected break value is 4.8% of the length of fiber as per the specifications given by supplier (Saint Gobian and Hexcel Corporation), whereas the length of E-glass fiber is 5 mm and elongation to break is 4.7% of the length of the fiber. Coefficient of friction (μ) is the ratio of frictional force to the normal load. Values of friction, normal load, and hardness are given in Table 4. These theoretical values are compared with the values obtained from experimental results conducted under similar operating conditions. Table 5 presents a

Table 4. Calculation of theoretical specific wear rate of glass fiber-reinforced epoxy composites.

Expt. no.	Fiber loading (wt.%)	Friction force (F) (long fiber)	Friction force (F) (short fiber)	Hardness (long fiber)	Hardness (short fiber)	Normal load (N)	Ws_{th} (Long fiber)	Ws_{th} (short fiber)
1	10	14	8	40.67	28.00	20	0.03586	0.03039
2	20	14	14	25.67	29.33	40	0.05682	0.05077
3	30	19	15	26.00	20.67	60	0.07612	0.07720
4	40	38	17	34.33	28.00	80	0.11530	0.06458
5	50	30	28	36.67	36.00	100	0.08521	0.08274
6	10	6	9	40.67	28.00	40	0.07683	0.01709
7	20	20	16	25.67	29.33	60	0.05410	0.03869
8	30	40	34	26.00	20.67	80	0.12019	0.13120
9	40	35	21	34.33	28.00	100	0.08496	0.06380
10	50	3	3	36.67	36.00	20	0.04261	0.04432
11	10	25	19	40.67	28.00	60	0.02134	0.02406
12	20	33	21	25.67	29.33	80	0.06695	0.03808
13	30	16	14	26.00	20.67	100	0.03895	0.04323
14	40	3	3	34.33	28.00	20	0.03641	0.04559
15	50	22	21	36.67	36.00	40	0.15623	0.15514
16	10	25	23	40.67	28.00	80	0.01601	0.02184
17	20	45	40	25.67	29.33	100	0.07304	0.05825
18	30	4	4	26.00	20.67	20	0.04807	0.06176
19	40	12	15	34.33	28.00	40	0.07282	0.11398
20	50	20	14	36.67	36.00	60	0.09471	0.06895
21	10	25	39	40.67	28.00	100	0.01280	0.02963
22	20	3	4	25.67	29.33	20	0.02434	0.029016
23	30	15	13	26.00	20.67	40	0.09014	0.10036
24	40	35	25	34.33	28.00	60	0.14159	0.12664
25	50	22	22	36.67	36.00	80	0.07812	0.08126

comparison between experimental results and theoretical results. The errors in experimental results with theoretical results for bidirectional glass fiber-reinforced epoxy composites lie in the range 0–15% (Table 5), whereas for chopped glass fiber-reinforced epoxy composites the range is 0–10% error (Table 5).

4.7. *ANOVA and the effects of factors for bidirectional/chopped glass fiber composites*

In order to find out statistical significance of various factors like sliding velocity, fiber loading, normal load, sliding distance, and abrasive size on specific wear rates of the bidirectional and chopped glass fiber-reinforced epoxy composites, ANOVA is performed based on Taguchi experimental results. Tables 6 and 7 show the results of the ANOVA with the specific wear rate of bidirectional and chopped glass-epoxy-based composites taken in this investigation. This analysis is undertaken for a level of confidence of significance 5%. The last column of the table indicates that the main effects are highly significant (all have very small p-values).

From Table 6, it can be observed for bidirectional glass-epoxy-based composites that normal load ($p = 0.094$), abrasive size ($p = 0.110$), sliding distance ($p = 0.476$), and sliding velocity ($p = 0.266$) have great influence on specific wear rate. However, fiber loading ($p = 0.027$) shows less significant contribution on specific wear rate of the composites.

Table 5. Comparison of theoretical and experimental specific wear rate of glass fiber-reinforced epoxy composites.

Expt. no.	Fiber loading (wt.%)	Ws_{th} (long fiber)	$Ws_{expt.}$ (long fiber)	Error (long fiber)	Ws_{th} (short fiber)	$Ws_{expt.}$ (short fiber)	Error (short fiber)
1	10	0.03586	0.03952	10.21	0.03039	0.03124	2.80
2	20	0.05682	0.06396	12.57	0.05077	0.04843	4.61
3	30	0.07612	0.07448	2.15	0.07720	0.07324	5.13
4	40	0.11530	0.10306	10.62	0.06458	0.05962	7.68
5	50	0.08521	0.09104	6.84	0.08274	0.08738	5.61
6	10	0.07683	0.06810	11.36	0.01709	0.01672	2.17
7	20	0.05410	0.06119	13.11	0.03869	0.03912	1.11
8	30	0.12019	0.12730	5.92	0.13120	0.14140	7.77
9	40	0.08496	0.09359	10.16	0.06380	0.05954	6.68
10	50	0.04261	0.03962	7.02	0.04432	0.04105	7.38
11	10	0.02134	0.02277	6.70	0.02406	0.02591	7.69
12	20	0.06695	0.05918	11.61	0.03808	0.03554	6.67
13	30	0.03895	0.03718	4.54	0.04323	0.04605	6.52
14	40	0.03641	0.03552	2.44	0.04559	0.04226	7.30
15	50	0.15623	0.16520	5.74	0.15514	0.14690	5.31
16	10	0.01601	0.01469	8.24	0.02184	0.01974	9.62
17	20	0.07304	0.06749	7.60	0.05825	0.05404	7.23
18	30	0.04807	0.04537	5.62	0.06176	0.05763	6.69
19	40	0.07282	0.06805	6.55	0.11398	0.11832	3.81
20	50	0.09471	0.08805	7.03	0.06895	0.07043	2.15
21	10	0.01280	0.01343	4.92	0.02963	0.02745	7.36
22	20	0.02434	0.02249	7.60	0.029016	0.02672	7.91
23	30	0.09014	0.08023	10.99	0.10036	0.09312	7.21
24	40	0.14159	0.13412	5.28	0.12664	0.11688	7.71
25	50	0.07812	0.06980	10.65	0.08126	0.07595	6.53

Table 6. ANOVA table for specific wear rate (long glass fiber).

Source	DF	Seq SS	Adj SS	Adj MS	*F*	*P*
A	4	70.335	70.335	17.584	1.95	0.2725
B	4	333.420	333.420	83.355	9.26	0.0276
C	4	154.149	154.149	38.537	4.28	0.0963
D	4	38.372	38.372	9.593	1.07	0.4877
E	4	138.254	138.254	34.563	3.84	0.1127
Error	4	36.017	36.017	9.004		
Total	24	770.546				

Note: Where DF-Degree of freedom, Seq SS-Sequential sum of square, Adj SS-Adjacent sum of square. Adj MS-Adjacent sum of mean square, *F*-Variance, *P*-Test statistics (percentage contribution of each factor in overall performance to find out optimum specific wear rate).

Similarly, from Table 7, it can be observed for the chopped glass fiber-reinforced epoxy composites that normal load ($p = 0.011$), sliding velocity ($p = 0.138$), and sliding distance ($p = 0.046$) have great influence on specific wear rate. The remaining factors have a less significant effect on the specific wear rate of the composites. Therefore, from this analysis it is clear that chopped fiber-reinforced epoxy composites are more suitable for abrasive wear environment as compared to that of bidirectional glass-epoxy

Table 7. ANOVA table for specific wear rate (short glass fiber).

Source	DF	Seq SS	Adj SS	Adj MS	*F*	*P*
A	4	13.115	13.115	3.279	3.28	0.6969
B	4	421.874	421.874	105.468	105.468	0.000
C	4	61.431	61.431	15.358	15.37	0.0555
D	4	26.687	26.687	6.672	6.68	0.2323
E	4	120.588	120.588	30.147	30.18	0.0151
Error	4	3.996	3.996	0.999		
Total	24	647.691				

Note: Where DF-Degree of freedom, Seq SS-Sequential sum of square, Adj SS-Adjacent sum of square. Adj MS-Adjacent sum of mean square, *F*-Variance, *P*-Test statistics (percentage contribution of each factor in overall performance to find out optimum specific wear rate).

composites, comparatively for a structural application point of view bidirectional glass fiber-reinforced epoxy composites show better mechanical properties than chopped glass fiber-reinforced epoxy composites.

5. Conclusion

A theoretical and experimental calculation carried out on bidirectional as well as chopped E-glass fiber-reinforced epoxy composites to investigate the effect of parameters like sliding velocity, fiber loading, normal load, sliding distance, and abrasive size on specific wear rate of composites leads to following conclusion. The following points can be concluded as under:

(1) Mathematical model based on weight loss and specific wear rate of composites during three-body abrasion has been developed. To overcome the shortcoming of previous models, two new terms i.e. percentage of fiber reinforcement and length of fiber have been introduced in the new model. It has been established that the values obtained from the developed theoretical model are very close to that of experimental once.
(2) Fiber reinforcement on long and short glass fiber has a significant effect on mechanical properties of the composites. Mechanical properties such as tensile strength, flexural strength, ILSS, impact strength, and hardness increase with the increase in fiber loading from 10 to 50 wt.%.
(3) Steady state condition is applied to find minimum specific wear rate for sliding velocity and normal for particular wt.% fiber reinforcement keeping other parameters as constant. It has been observed that specific wear rate decreases with the increase in sliding velocity up to 40 wt.% fiber reinforcement and then further increases, whereas specific wear increases with the increase in normal load.
(4) In Taguchi experimental analysis it has been observed that for similar test conditions chopped glass-epoxy composites exhibit much lower wear rates than those by bidirectional composites. Therefore, chopped glass fiber is a better substitute for lower wear rates than that of bidirectional composites.
(5) Theoretical values of specific wear rate are calculated based on the developed model and further compared it with experimental specific wear rate values. The errors in experimental results with theoretical results for bidirectional glass

fiber-reinforced epoxy composites lie in the range 0–15%. Whereas for chopped glass fiber-reinforced epoxy composites the error is in the range of 0–10%.

(6) In future, the study can be extended to new polymer composites having different fiber/matrix combinations and the resulting experimental findings can be further analyzed.

References

[1] Fried K. Wear of reinforced polymers by different abrasive counterparts. In: Friedrich K, editor. Friction and wear of polymer composites. Amsterdam: Elsevier; 1986. p. 233–287.
[2] Ludema KC. Friction, wear, lubrication: a textbook in tribology. Boca Raton (FL): CRC Press LLC; 1996.
[3] Stachowiak GW, Batchelor AW. Engineering tribology. Oxford: Butterworth-Heinemann; 1998.
[4] Bartenex GM, Laurentev XX. Friction and wear of polymers. Amsterdam: Elsevier; 1981.
[5] Cirino M, Friedrich K, Pipes RB. The abrasive wear behavior of continuous fiber polymer composites. J. Mater. Sci. 1987;22:2481–2492.
[6] Friedrich K, Lu Z, Hager AM. Recent advances in polymer composites tribology. Wear. 1995;190:139–144.
[7] Chand N, Naik A, Neogi S. Three-body abrasive wear of short glass fibre polyester composite. Wear. 2000;242:38–46.
[8] Suresha B, Kumar KS, Seetharamu S, Kumaran PS. Friction and dry sliding wear behavior of carbon and glass fabric reinforced vinyl ester composites. Tribol. Int. 2010;43:602–609.
[9] Suresha B, Kunigal N, Kumar S. Investigations on mechanical and two-body abrasive wear behavior of glass/carbon fabric reinforced vinyl ester composite. Mater. Des. 2009;30:2056–2060.
[10] Sharma M, Rao IM, Bijwe J. Influence of fiber orientation on abrasive wear of unidirectionally reinforced carbon fiber–polyetherimide composites. Tribol. Int. 2010;43:959–964.
[11] Lu Z, Friedrich K, Pannhorst W, Heinz J. Wear and friction of a unidirectional carbon fiber-glass matrix composite against various counterparts. Wear. 1993;162–164:1103–1113.
[12] Chand N, Gautam KKS. Influence of load on abrasion of fly ash-glass fibre-reinforced composites. J. Mater. Sci. Lett. 1994;13:230–233.
[13] Cirino M, Friedrich K, Pipes RB. The abrasive wear behavior of continuous fiber polymer composites. J. Mater. Sci. 1987;22:235–247.
[14] Hutchings IM. Tribology: friction and wear of engineering materials. London: Edward Arnold; 1992.
[15] Rabinowicz E. Friction and wear of materials. New York: Wiley; 1965.
[16] Ratner SB, Ferverova II, RadyukevichOV, Lure EG. Connection between wear resistance of plastics and other mechanical properties. In: James DI, editor. Abrasion of rubber, Soviet Plast. London: Mac Laren; 1964;12:37.
[17] Agarwal BD, Broutman IJ. Analysis and performance of fiber composites. 2nd ed. New York: Wiley; 1990.
[18] Tensile properties of fiber–resin composites ASTM D 3039-76. American National standard; 1976.
[19] American Society for Testing and Materials (ASTM). Standard test method for apparent interlaminar shear strength for parallel fiber composites by short beam method ASTM D 2344-84. In: Annual book of ASTM standards. West Conshohocken (PA): ASTM; 1984. p. 15–17.
[20] American society for testing and materials (ASTM). Standard D 256-97, standard test methods for determining the pendulum impact resistance of notched specimens of plastic, 1999. Annual book of ASTM standards. Vol. 08.01. West Conshohocken (PA): ASTM; 1997. p. 1–20.
[21] Stokes VK. Random glass mat reinforced thermoplastic composites. Part IV: characterization of the tensile strength. Polym. Compos. 1990;11:354–367.
[22] Thomason JL, Vlug MA, Schipper G, Krikor HGLT. The influence of fibre length and concentration on the properties of glass fibre-reinforced polypropylene: Part 3. Strength and strain at failure. Composites Part A. 1996;27:1075–1084.

[23] Asri SM, Khalik AHPS. Utilization of oil palm fibres thermoplastic prepreg in polyester hybrid composites. In: Proceedings of 3rd National symposium on polymeric materials; Dec 30–31; Skudai; 2002. p.160–166.
[24] Nigel SJ, Brown JR. Flexural and interlaminar shear properties of glass reinforced phenolic composite. Composites Part A. 1998;29:939–946.
[25] Menard KP. Dynamic mechanical analysis. New York: Taylor & Francis; 2008.
[26] Kumar S, Satapathy BK, Patnaik A. Thermo mechanical correlations to erosion performance of short carbon fiber reinforced vinyl ester resin composites. Mater. Des. 2010;32:2260–2268.
[27] Kumar S, Satapathy BK, Patnaik A. Viscoelastic interpretations of erosion performance of short aramid fibre reinforced vinyl ester resin composites. J. Mater. Sci. 2011;46:7489–7500.